S. Afr. J. Chem., 2025, 79, 125–131
https://journals.co.za/content/journal/chem/

An Investigation of the Synergistic Influence of Surface Pipeline Temperature and Water Condensation Rate on Top-of-the-Line Corrosion of X65 Steel in a CO_2 Vapour Environment

Khalid Abdulhussain Mohammed

Oil and Gas Department, College of Engineering, University of Thi-Qar, Nasiriyah, Iraq.

ABSTRACT

Wet gases are typically produced and transported through carbon steel pipeline systems. The combination of corrosive gases and transportation conditions creates highly aggressive environments, often leading to recurring incidents of pipeline corrosion failure. This study investigated the corrosion rate on the internal upper surface of the X65 carbon steel pipeline under static conditions, where gas flow is dominated by natural convection. To replicate realistic field conditions, a novel apparatus was designed to measure condensation rates, water droplet lifespan, and top-of-line corrosion (TLC) rates across a wide range of steel surfaces and gas temperatures. Surface morphology was characterized using SEM imaging to evaluate the corrosion morphology and identify the types of corrosion deposits. The findings reveal that when the surface temperature is at or below 30°C, TLC is primarily governed by the water condensation rate and surface temperature. However, at surface temperatures above 30°C, the condensation rate becomes the dominant controlling parameter. In the top of the line (TOL) scenario, the lifetime of the condensed water droplet plays a critical role in determining the corrosion rate. The results further demonstrate that the droplet lifespan affects the formation and precipitation of the $FeCO_3$ film, which in turn influences corrosion behavior.

KEYWORDS

top of line corrosion, gas temperature, steel temperature, water condensation rate

Received 29 April 2025, revised 16 July 2025, accepted 1 August 2025

INTRODUCTION

Crude oil and natural gas are typically transported through carbon steel pipelines, and this stage in oil and gas production presents significant corrosion risks. The produced oil is typically unprocessed and contains a combination of gas, brine, and solids. The presence of various dissolved gases, such as carbon dioxide (CO_2), hydrogen sulphide (H_2S), and organic acids (e.g., acetic and formic acid), in combination with brine, can lead to severe corrosion problems at the internal surfaces of carbon steel pipelines.[1]

One specific form of corrosion associated with wet gas production is known as Top-of-Line Corrosion (TLC). TLC was first discovered in the 1960s and became widely recognized in the context of wet gas transportation, particularly when significant heat exchange occurs between the transported gas and the adjacent environment. If the flow regime of multiphase fluids (gas/liquid) is stratified, the saturated water vapor can condense at the inner wall of the pipeline due to the temperature differences between the outside environment and the produced fluid.[1] The droplets of condensed water can contain dissolved gases, particularly CO_2, H_2S, and corrosive species such as organic acids, forming a corrosive chemical solution with properties significantly different from those flowing at the bottom of the pipeline.

Figure 1 clearly distinguishes between the two primary corrosion mechanisms in wet gas systems: Top-of-the-Line (TOL) corrosion results from the condensation of water vapor on the inner upper surface of the pipeline due to temperature gradients between the gas phase and the pipeline wall. The resulting droplets create localized corrosive environments unique to the gas-phase condensate. Bottom-of-the-Line (BOL) corrosion, by contrast, occurs in the stratified liquid layer at the bottom of the pipe, where the aqueous phase is in continuous contact with the steel surface. The chemistry of this bulk liquid can differ significantly from the condensate droplets at the top.

The condensed liquid in the pipeline has a pH value ranging from 3 to 4 due to the absence of minerals and bases in the solution.[2] The acidic environment can lead to a very fast corrosion process, which in turn causes costly accidents, pipeline failures, production loss, and environmental damage. Furthermore, since most corrosion inhibitors are non-volatile, preventing them from effectively reaching the upper surface of the pipeline in stratified flow conditions, this complicates the application of inhibitors to mitigate TLC.[1]

Since the first reported case in 1960 in France,[3] several laboratory studies on TLC have been conducted, and numerous predictive

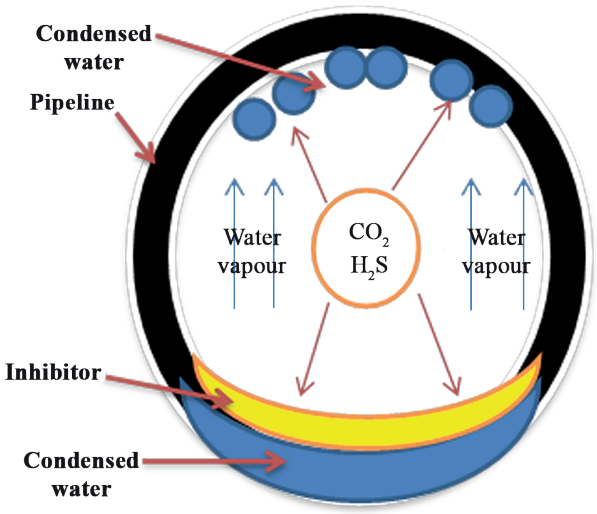

Figure 1: Schematic of corrosion mechanisms in wet gas pipelines showing the distinction between Top-of-the-Line (TOL) and Bottom-of-the-Line (BOL) corrosion.

*To whom correspondence should be addressed
Email: dr.khalid@utq.edu.iq

ISSN 1996-840X Online / South African Chemical Institute / http://saci.co.za/journal

https://doi.org/10.17159/0379-4350/2025/v79a13

models have been proposed to improve the understanding of TLC.[1,2,4-10] Most of these models consider the influences of water condensation rate (WCR) and gas temperature (T_g); however, when calculating WCR, they primarily account for the surface temperature (T_s) through heat transfer via the pipeline walls. These factors govern the dissolution process of the steel surface and determine whether the condensed water is saturated with iron carbonate ($FeCO_3$). This saturation facilitates and enhances the process of iron carbonate precipitation onto the steel surface, forming a protective layer of iron carbonate that can hinder further steel dissolution.[1, 4] Consequently, identifying the kinetics behavior of the formation of iron carbonate film, including when it forms or does not form, is a crucial step to determining overall corrosion rates and the possibility of localized corrosion occurring. The thermodynamics governing the formation of iron carbonate film and steel surface dissolution are controlled by T_s, T_g, and WCR.[1,4]

Although previous studies have extensively investigated the mechanisms of top-of-line corrosion (TLC), their focus predominantly revolved around specific variables like the water condensation rate (WCR) and the influence of gas temperatures (T_g) on corrosion rates. These studies have laid significant groundwork, but often relied on assumptions or limited experimental conditions.[4, 11-13]

This study aims to address these gaps by employing a novel experimental setup and conducting a comprehensive analysis. Isolating the most influential factors remains one of the most challenging steps in understanding the TLC mechanism. This research presents a TLC setup designed to simultaneously measure the actual surface and gas temperature, collect the condensed water, and determine the water condensation rate. This setup allowed for a clear distinction between the individual impacts of two interrelated parameters, water condensation rate (WCR) and surface temperature (T_s), on the TLC. Additionally, the thermodynamics and kinetics of $FeCO_3$ scale formation at the top-of-line are examined using SEM imaging and X-ray diffraction (XRD).

NOVELTY IN EXPERIMENTAL SETUP

Singer et al. introduced a setup that explored TLC under sour conditions using carbon dioxide and hydrogen sulfide environments.[1] However, their apparatus did not simultaneously account for the dynamic interplay between surface temperature (T_s) and water condensation rate (WCR). In contrast, the innovative design developed here measures these parameters concurrently, providing a more comprehensive view of their synergistic effects on TLC. This dual-factor approach enables a more precise understanding of how temperature gradients influence both condensation dynamics and corrosion mechanisms.

Islam et al. primarily focused on condensation corrosion at moderate surface temperatures and its relationship with $FeCO_3$ precipitation kinetics.[4] While their study provided valuable insights, it lacked a systematic exploration of higher temperature ranges and their impact on droplet behavior. The present work bridges this gap by extending the temperature range to include higher T_s values, where unique phenomena such as the decoupling of WCR influence at T_s > 30°C were observed.

EXPERIMENTAL METHODS

Experimental TLC Test Cells

Experiments at atmospheric pressure were conducted using glass cells, each cell containing two X65 carbon steel coupons. Figure 2 illustrates a photograph of the TLC cell employed in the experiments.

The standard elemental composition of the X65 samples is summarized in Table 1. Each sample was machined into a cylindrical form with a diameter of 25 mm and a thickness of 10 mm. A central hole, 2 mm in diameter and 9 mm in depth was drilled into each sample, leaving 1 mm from the bottom surface of the sample to accommodate a temperature probe for the measurement of the surface temperature (T_s). During the test, the X65 coupons were flush-mounted into the lids of the glass cells, and oil was dropped into the hole to ensure consistent and stable surface temperature measurements.

To control the water condensation process, a 10 mm diameter spiral copper coil was placed around the holder, through which water was circulated to cool the sample and achieve the desired surface temperature (T_s). The target gas temperature (T_g) was achieved by heating the bottom solution using a hot plate. This design created an in-situ condensation process that mimics field pipeline conditions.

The aqueous solution consists of CO_2-saturated distilled water, which had been purged with CO_2 gas for at least 12 hours prior to the start of each experiment to ensure minimum oxygen content in the water. Additionally, during the experiments, CO_2 gas was continuously bubbled into the solution to maintain complete saturation.

For WCR and pH measurements of the condensate, condensed water was collected by a small funnel installed beneath the test sample and immediately transferred to a sealed, CO_2-saturated collection container. WCR measurements were carried out twice daily throughout the test period, which lasted 168 hours.

The mass loss technique for measuring the rate of corrosion was employed in this study due to difficulties with performing electrochemical corrosion measurements under top-of-line conditions over extended periods. This method imposes a limitation because it provides integrated results, unlike electrochemical tests, which give real-time corrosion rates. However, the transient behavior was investigated by regular measurements taken after 24, 48, 72, 96, 120, 144, and 168 hours.

To ensure the accuracy and reliability of the results, the experiments were repeated at least three times. Error bars represent the minimum and maximum corrosion rate values under each test condition are

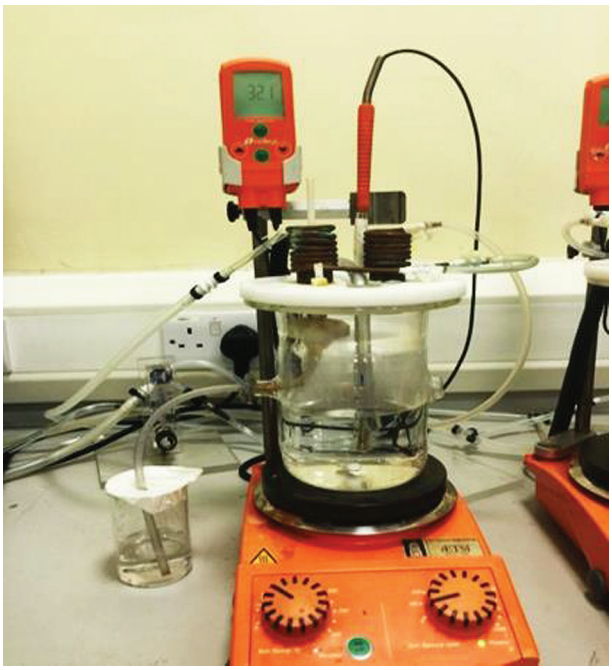

Figure 2: Photo of the TLC setup.

Table 1: X65 Carbon steel composition (wt.%).[2]

C	Si	Mn	P	S	Cr	Mo	Ni	Cu	Sn	Al	B	Nb	Ti	V	Fe
0.12	0.18	1.27	0.008	0.002	0.11	0.17	0.07	0.12	0.008	0.022	0.005	0.054	0.001	0.057	Bal

shown in the graphs. The test matrix for the experiments is presented in Table 2.

Experimental Measurements of Condensation and Corrosion Rates

Throughout the pre-test preparations, the exposed surfaces of samples were polished using grit sandpaper up to 1200 grit, then washed with isopropanol solution and dried with a heat gun. After that, the side and the upper face of each sample were coated carefully with a thin layer of protective lacquer.

The samples were then wet-grounded and weighed using a high-precision digital scale with a resolution of 0.05 mg to measure their initial mass (m_1) before being mounted into the lid. The required inner surface temperature was achieved and maintained using a cooling chamber. To accomplish this, it was possible to control the temperature at which cold water circulates through copper coils around the sample. The water condensation rates were calculated using the following equation:

$$WCR = \frac{V_w \rho_w}{S_t t_c} \quad (1)$$

where, WCR = water condensation rate, (g/m².s); V_W= condensed water volume, (ml); ρ_W = water density, (g/cm³); t_c = duration time over which the condensate is collected, (s); S_t = sample surface area, (m²).

Following each corrosion rate measurement, samples were taken and rinsed with distilled water, then ethanol, and gently dried using an air gun. The samples were then weighed to record their post-exposure mass (m²). Corrosion products were removed from the surface using Clarke's solution and prepared according to ASTM Standard G1-03.[14] The solution consisted of 20 g antimony trioxide, 50 g stannous chloride, and 1000 ml of hydrochloric acid. Corrosion rates were calculated based on the weight loss method, using the following equation.[2]

$$CR = \frac{87600(m_1 - m_2)}{\tilde{n}_{Fe} A t} \quad (2)$$

where, CR is the corrosion rate, mm/y; $(m_1 - m_2)$ is the mass loss, grams; ρ_{Fe} is the carbon steel density = 7.85 g/cm³; A is the surface area exposed to corrosion, cm²; t is the duration of the test time, in hours.

Table 2: Test matrix used to assess the effect of T_g, T_s, and WCR on TLC

Material	Carbon steel (X65)
Total pressure	1 bar
Gas temperature)	30-60°C
Inner steel temperature	5-52 °C
Test duration	168 hrs
pH	5.0-5.93

EXPERIMENTAL RESULTS AND ANALYSIS

The results are subdivided into two main categories: water condensation rate and weight loss corrosion results.

Water Condensation Rates

Figure 3 shows the in-situ average WCR measurements across a range of gas (T_g) and steel surface (T_s) temperatures over a test period of 168 hours.

According to the results of these experiments, the maximum temperature difference between bulk gas and the steel surface of 45°C was observed when T_g = 60°C and T_s = 15°C, resulting in a WCR of 1.70 mL/m².s. Conversely, the minimum WCR of 0.17 mL/m².s was recorded at the lowest temperature difference of 5°C when T_g is 30°C and T_s is 25°C.

It is clear from the WCR measurements that the temperature difference between the bulk gas and the steel temperature is a critical factor influencing the rate of condensation. This relationship can be attributed to the fact that when temperatures are increased, a higher rate of condensation is also achieved due to an increase in humidity, which enhances heat and mass transfer, as described by Nusselt's theory of condensation.[2,15,16]

Average Corrosion Rates

The two main parameters, steel surface temperature and water condensation rate are considered the primary factors controlling the

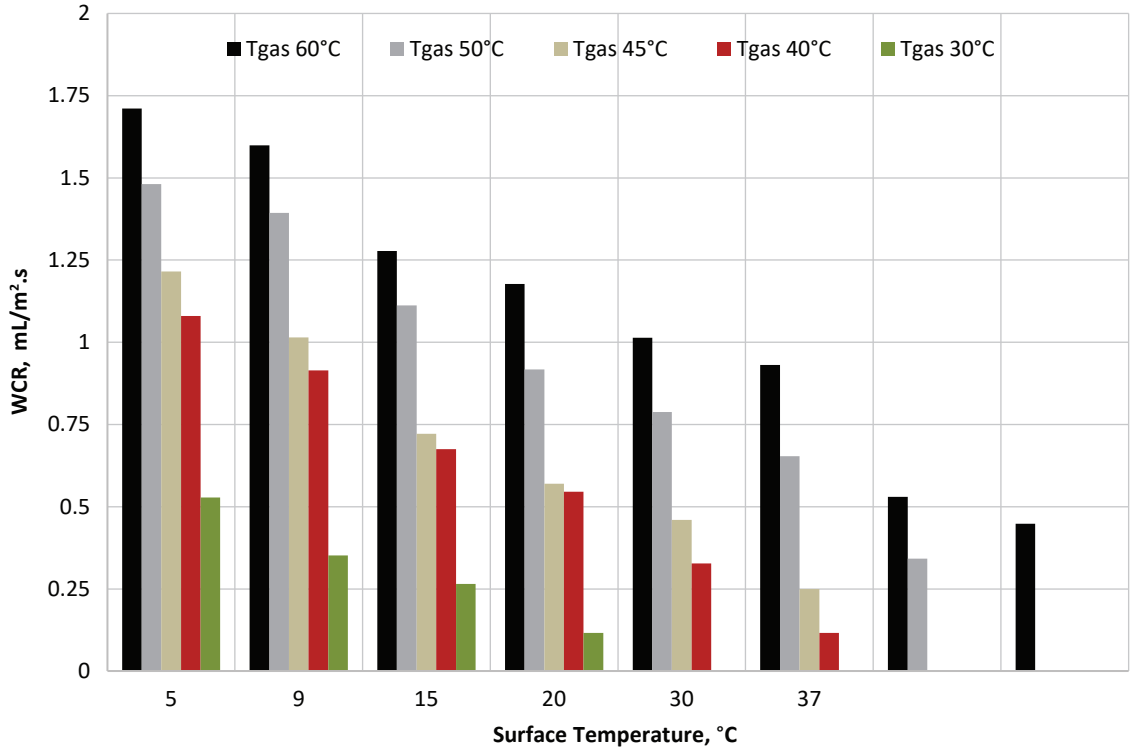

Figure 3: The relationship between the condensation rates and surface temperatures at different gas temperatures.

corrosion threat on the top surface of the pipeline.[13,17] Consequently, these parameters were systematically varied to assess their influence on the average corrosion rate for X65 carbon steel over time.

Surface Temperature Effect

Across all corrosion experiments, two notable trends were observed. First, the average corrosion rate significantly increased over time. Second, after an initial period of stability, the values of the average corrosion rate exhibited a gradual decline. The results of both scenarios are presented in Figure 4.

When T_g is 40°C, the average corrosion rate increases with time at T_s of 15 and 30°C, as shown in Figure 4 (a). This behavior is attributed to the formation of an iron carbide layer (Fe_3C), a corrosion product which is commonly observed in corrosion products in the CO_2 corrosion process of low alloy carbon steels,[18] being present on the sample surface after exposure, as confirmed by SEM images in Figure 5 and Figure 6 (a).

Fe_3C is often left on the metal surface after a corrosion process because it is more difficult to dissolve in an aqueous solution than the ferrite phase (α-Fe).[18] The subsequent reduction in the corrosion rate is associated with a decrease in WCR, observed at T_s = 38°C and T_g = 40°C, where the corrosion rate began to decline after 96 hours. A similar trend was observed at T_g was 50°C, as illustrated in Figure 4 (b), although a more pronounced increase in the average corrosion rate was noted at T_s = 15°C and 30°C, followed by a reduction at T_s = 38°C.

It is well known that Fe_3C is an electrochemical conductor and acts as a cathodic site when hydrogen ions are reduced. The iron carbide and ferrite phases affect the steel microstructure, where iron carbide can accelerate corrosion, and ferrite is subject to dissolution, resulting in an eroded surface. A galvanic cell is formed between the corroded ferrite, which acts as the anode, and iron carbide, which acts as a cathode. As the corrosion process continues, more Fe_3C forms, leading to an enhancement in cathodic reactions and, consequently, higher average corrosion rates.[19-21]

All experiments were classified as either $FeCO_3$ film-forming or non-forming based on ex-situ analysis of sample surfaces and corrosion rate results at the end of the 168-hour test period.

The results indicate that protective films formed on sample surfaces when certain conditions were met during the experiments. Representative SEM images illustrating the visual appearance of the surface with and without the $FeCO_3$ film are presented in Figure 6. Additionally, the XRD pattern shown in Figure 6 (c) confirms that the corrosion product observed in Figure 6(b) is $FeCO_3$.

WCR Effect

The influence of T_s and WCR on top-of-line corrosion (TLC) is presented in Figure 7. The corrosion rate is expected to increase significantly with the WCR due to the more frequent renewal of water droplets at higher condensation rates.

A significant increase in WCR, from 0.31 to 1.71 mL/m².s, was observed at low surface temperatures of 15°C when the gas temperature increased from 30°C to 60°C. Even though the WCR increased more than fivefold, this change did not lead to a substantial increase in the corrosion rate.

At higher surface temperatures, such as 30°C and 38°C, WCR had a greater impact on the corrosion rate. For instance, an increase in WCR from 0.29 to 1.34 mL/m².s at 30°C resulted in an increase in the average corrosion rate from 0.71 to 1.52 mm/y. Similarly, when the surface temperature was 38°C, the WCR rose from 0.12 to 0.91 mL/m².s, corrosion rates increased substantially from 0.25 to 1.22 mm/y. These results indicate that a higher WCR is a critical factor contributing to increasing the corrosion rate at higher surface temperatures.

Based on these obtained results and the previous observation, it can be deduced that under low-temperature conditions, the corrosion rate is essentially dependent upon steel temperature and is relatively insensitive to the water condensation rate (WCR). This behavior is due to the lower rate of iron dissolution at reduced surface temperatures, resulting in an extremely low concentration of Fe^{2+} ions in the condensed liquid. Consequently, supersaturation levels remain very low, leading to negligible accumulations of corrosion products on steel surfaces.

Under these conditions, the corrosion reaction is controlled by the steel temperature rather than the gas temperature. Additionally, at low WCRs, droplets can remain attached to the top inner surface

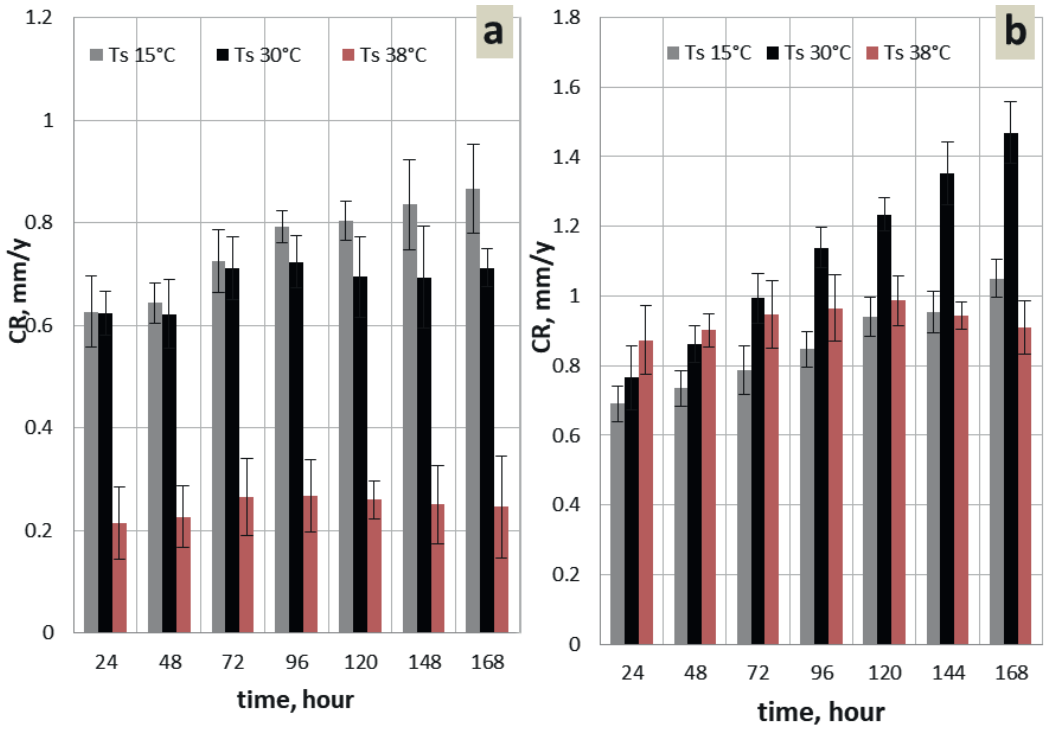

Figure 4: Influence of surface temperature on average corrosion rates at (a) T_g = 40°C and (b) T_g = 50°C.

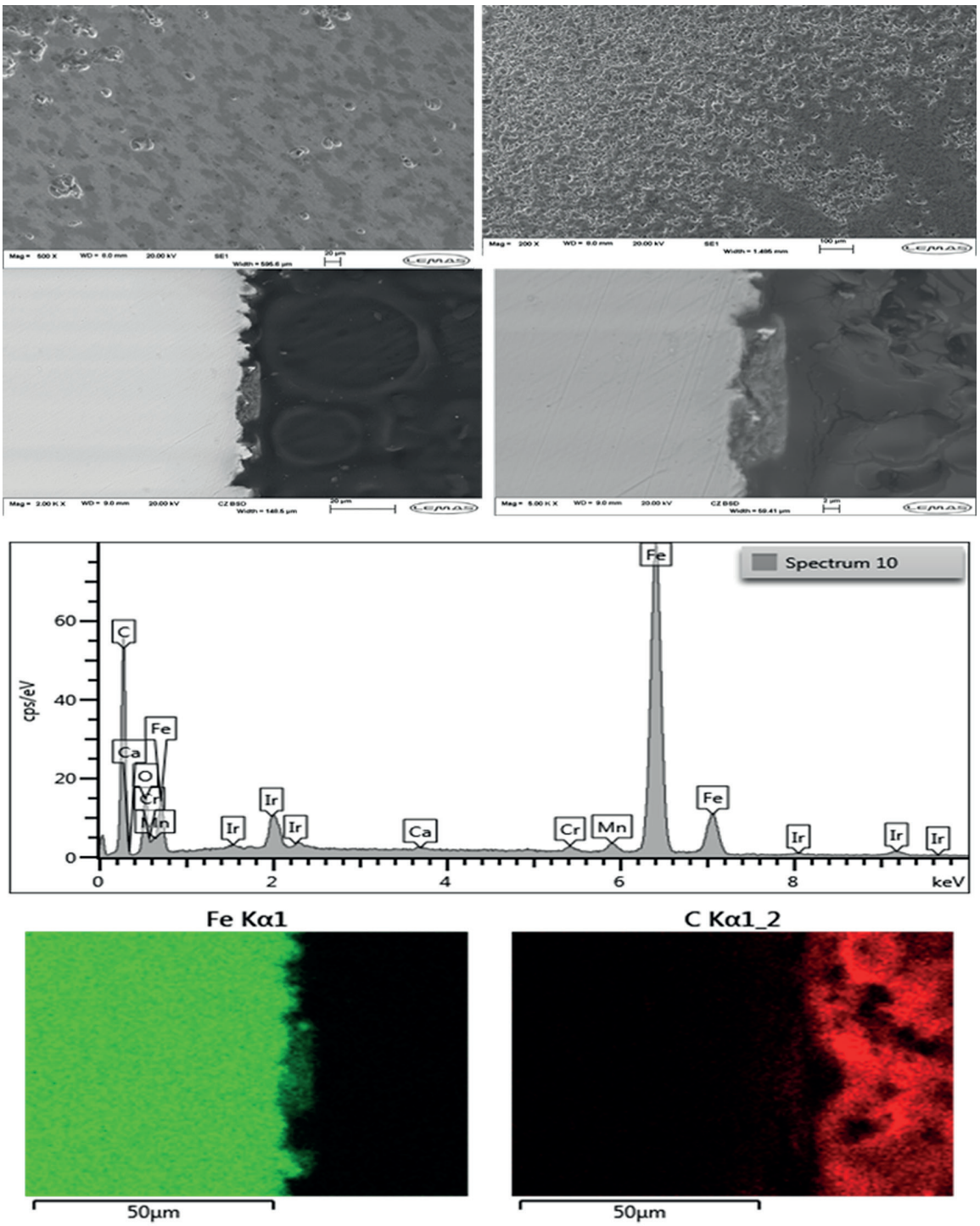

Figure 5: SEM images, EDS spectra, and cross-section analysis of corrosion product formed on the coupon surface after 168 hours of exposure at (T_g = 50°C and T_s = 30°C).

for extended periods, allowing conditions to become favourable for the formation of iron carbonate scales within droplets. Therefore, the combination of a high surface temperature and prolonged droplet lifetime promotes the formation of a protective iron carbonate film on the surface.

CONCLUSIONS

In this study, water condensation and inner surface temperature were systematically varied over time to assess their effect on the top-of-the-line corrosion of carbon steel in a CO_2_rich environment. Based on the experimental findings, the following conclusions can be drawn:

- A critical temperature threshold of the pipeline surface (Ts ≥ 30°C) was identified, above which corrosion rate is predominantly governed by surface temperature and WCR. Whereas, below this temperature, WCR has minimal impact on TLC rates
- At lower surface temperatures, no substantial differences were noted in the corrosion rates, even though WCRs increased. Whereas, at high sample surface temperature, increasing WCR significantly accelerates corrosion.
- Droplet lifetime plays a critical role in $FeCO_3$ film formation under TOL conditions. Short-lived droplets may not allow film formation even at high supersaturation.
- $FeCO_3$ film formation and precipitation behavior differ between TOL and BOL conditions. While high supersaturation typically promotes film formation at BOL, TOL conditions require sustained droplet presence on the surface.

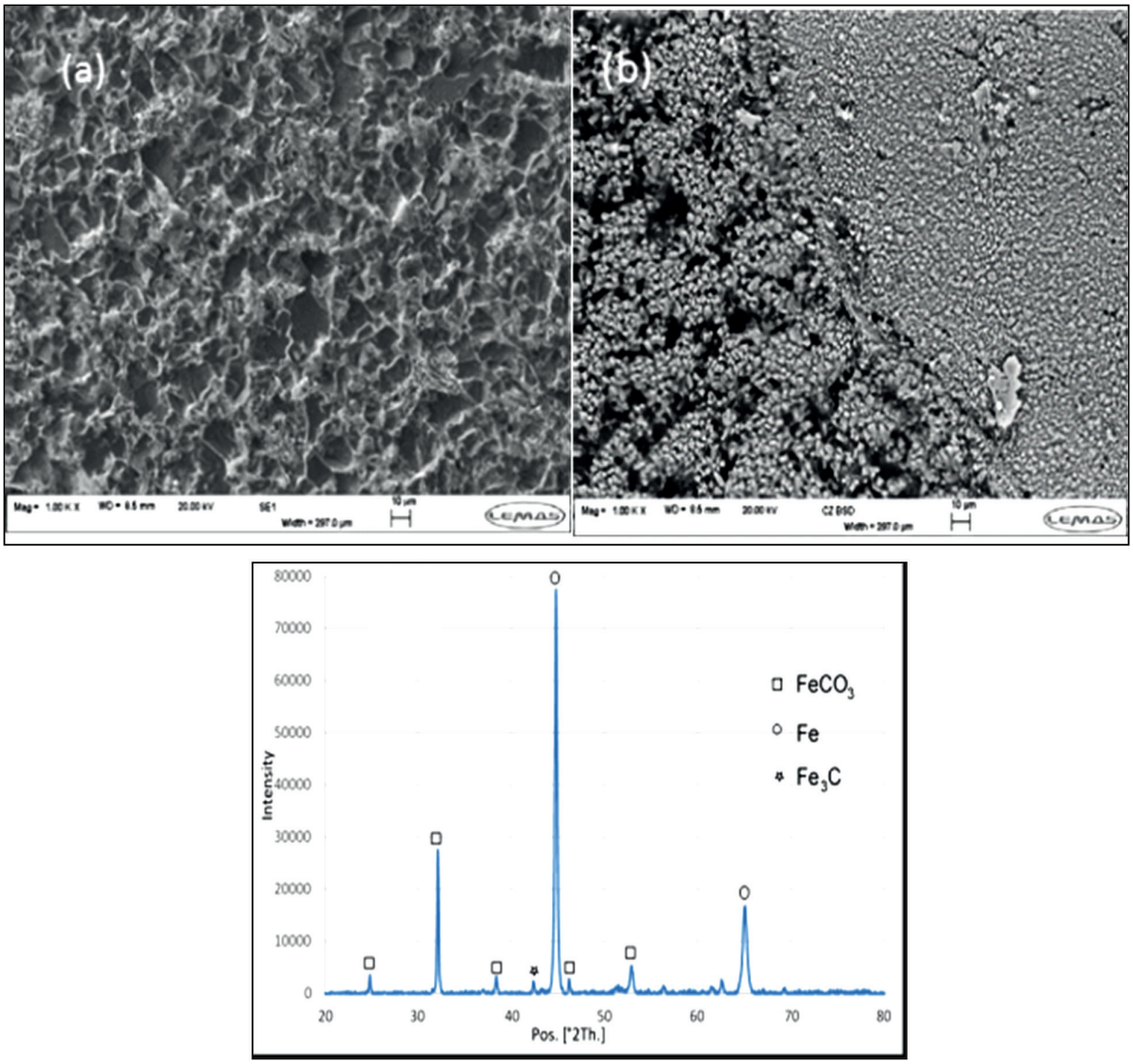

Figure 6: SEM images of selected sample surfaces after 168 hours of exposure: (a) Tg = 50°C and Ts = 15°C, showing Fe_3C formation; (b) Tg = 50°C and Ts = 38°C, showing the partial coverage of the steel surface by $FeCO_3$; (c) XRD pattern of corrosion products formed on the X65 sample.

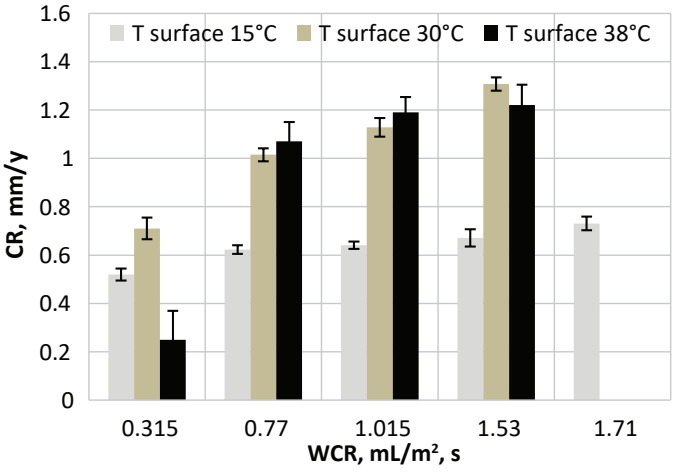

Figure 7: Influence of water condensation rate (WCR) on top-of-line corrosion rate (TLC) at different surface temperatures.

These findings highlight the complex interdependence of Ts, WCR, and droplet behavior in governing TLC mechanisms and have practical implications for corrosion prediction and mitigation in wet gas pipelines.

ACKNOWLEDGMENTS

The author is grateful to the Petroleum and Gas Engineering Department and the University of Thi-Qar for their financial and scientific support.

AUTHOR CONTRIBUTIONS

The author confirms sole responsibility for all aspects of the study, including conceptualization, methodology, investigation, writing, and final review and editing.

CONFLICT OF INTEREST

The author declares that there are no conflicts of interest regarding the publication of this manuscript.

DECLARATION OF GENERATIVE AI AND AI-ASSISTED TECHNOLOGIES

Not applicable.

ORCID ID

Khalid A. Mohammed: https://orcid.org/0000-0002-0207-3479

REFERENCES

1. Singer M, Al-Khamis J, Nešić S. Experimental study of sour top-of-the-line corrosion using a novel experimental setup. Corrosion. 2013;69(6):624–638. https://doi.org/10.5006/0738E
2. Mohammed KA. Experimental and theoretical investigation of top-of-the-line corrosion in CO_2 gas and oil environments. PhD thesis, University of Leeds; 2018. https://etheses.whiterose.ac.uk/id/eprint/20479/
3. Jenkins A, Gilbert I. Development of a Top-of-Line Corrosion Inhibitor and a Top-of-Line Corrosion Test Method. Proceedings of the CORROSION 2012. CORROSION 2012. Salt Lake City, Utah, USA; March 11–14, 2012. pp 1–12). AMPP. https://doi.org/10.5006/C2012-01275
4. Islam MM, Pojtanabuntoeng T, Gubner R. Condensation corrosion of carbon steel at low to moderate surface temperature and iron carbonate precipitation kinetics. Corros Sci. 2016;111:139–150. https://doi.org/10.1016/j.corsci.2016.05.006
5. Méndez C, Singer M, Camacho A, Hernández S, Nesic S, Gunaltun Y, Joosten M, Sun Y, Gabbetta P. Effect of acetic acid, pH and MEG on the CO_2 top of the line corrosion. Corrosion. 2005;2005:1–27. https://doi.org/10.5006/C2005-05278
6. Egab K, Mohammed KA, Okab AK, Oudah S. Numerical study of condensation heat transfer and droplet dynamics on different wetting surfaces of gas transportation pipelines. IOP Conference Series: Materials Science and Engineering, Volume 928, 2nd International Scientific Conference of Al-Ayen University (ISCAU-2020) 15–16 July 2020, Thi-Qar, Iraq. Article 022105. https://doi.org/10.1088/1757-899X/928/2/022105
7. Neshati J, Saremi M, Mashhadi G. A new approach in top-of-line corrosion studies in CO2/H2S environment. Corros Eng Sci Technol. 2023;58(8):723–733. https://doi.org/10.1080/1478422X.2023.2250156
8. Stack MM, Abdulrahman GH. Mapping erosion–corrosion of carbon steel in oil–water solutions: Effects of velocity and applied potential. Wear. 2012;274–275:401–413. https://doi.org/10.1016/j.wear.2011.10.008
9. Albrahim I, Al-Abbas F, Costa RS, Debruyn H, Al-Saif O. Probe into water chemistry effects on internal corrosion risk for sour gas pipelines. J Pipeline Syst Eng Pract. 2024;15(2):04024002. https://doi.org/10.1061/JPSEA2.PSENG-1447
10. Al-Moubaraki AH, Obot I. Top of the line corrosion: causes, mechanisms, and mitigation using corrosion inhibitors. Arab J Chem. 2021;14(5):103116. https://doi.org/10.1016/j.arabjc.2021.103116
11. Yaakob N, Singer M, Young D. Top of the line corrosion behavior in highly sour environments: effect of the gas/steel temperature. Proceedings of the CORROSION 2014. CORROSION 2014. San Antonio, Texas, USA; March 9–13, 2014. AMPP. pp 1–10. https://doi.org/10.5006/C2014-3807
12. Singer M, Hinkson D, Zhang Z, Wang H, Nešić S. CO_2 top-of-the-line corrosion in the presence of acetic acid: a parametric study. Corrosion. 2013;69(7):719–735. https://doi.org/10.5006/0737.
13. Singer M, Nesic S, Gunaltun Y. Top of the line corrosion in presence of acetic acid and carbon dioxide. Proceedings of the CORROSION 2004. CORROSION 2004. New Orleans, Louisiana, USA; March 27–April 1, 2004. AMPP. pp. 1–20. https://doi.org/10.5006/C2004-04377
14. Metals ACG-Co. Standard practice for preparing, cleaning, and evaluating corrosion test specimens. West Conshohocken: ASTM International; 2011. https://doi.org/10.1520/G0001-03R17E01
15. Rose JW. Enhanced condensation heat transfer. JSME Int. J. Ser. B. 2006; 49(3):626–635. https://doi.org/10.1299/jsmeb.49.626
16. Stephan K, Green CV. Heat transfer in condensation and boiling. Springer; 1992. https://doi.org/10.1007/978-3-642-52457-8
17. Nyborg R, Dugstad A. Top of line corrosion and water condensation rates in wet gas pipelines. Proceedings of the CORROSION 2007. CORROSION 2007. Nashville, Tennessee, USA; March 11–15, 2007. AMPP. pp 1–10. https://doi.org/10.5006/C2007-07555
18. Vitse F. Experimental and theoretical study of the phenomena of corrosion by carbon dioxide under dewing conditions at the top of a horizontal pipeline in the presence of non-condensable gas. PhD Thesis, Ohio University, USA; 2002.
19. López DA, Simison S, De Sanchez S. The influence of steel microstructure on CO 2 corrosion. EIS studies on the inhibition efficiency of benzimidazole. Electrochim Acta. 2003;48(7):845–854. https://doi.org/10.1016/S0013-4686(02)00776-4
20. Eliyan FF, Alfantazi A. On the theory of CO 2 corrosion reactions–Investigating their interrelation with the corrosion products and API-X100 steel microstructure. Corros Sci. 2014;85:380–393. https://doi.org/10.1016/j.corsci.2014.04.055
21. Gao M, Pang X, Gao K. The growth mechanism of CO2 corrosion product films. Corros Sci. 2011;53(2):557–568. https://doi.org/10.1016/j.corsci.2010.09.060